

Three-Dimensional Fermi-Liquid Ground State in the Quasi-One-Dimensional Cuprate $\text{PrBa}_2\text{Cu}_4\text{O}_8$

N. E. Hussey,¹ M. N. McBrien,¹ L. Balicas,² J. S. Brooks,² S. Horii,³ and H. Ikuta⁴

¹*H. H. Wills Physics Laboratory, University of Bristol, Tyndall Avenue, Bristol, BS8 1TL, United Kingdom*

²*National High Magnetic Field Laboratory, Florida State University, Tallahassee, Florida 32306*

³*Department of Applied Chemistry, University of Tokyo, Tokyo 113-8656, Japan*

⁴*Center for Integrated Research in Science and Engineering, Nagoya University, Chikusa-ku, Nagoya, 464-8603, Japan*

(Received 20 November 2001; published 5 August 2002)

The interchain resistivity of $\text{PrBa}_2\text{Cu}_4\text{O}_8$ has been measured in high magnetic fields up to 30 T. Coherent interchain transport at low temperatures is destroyed by a large magnetic field applied perpendicular to the CuO chains. Comparisons with quasiclassical transport theory provide strong experimental support for a three-dimensional Fermi-liquid ground state in $\text{PrBa}_2\text{Cu}_4\text{O}_8$, despite extreme anisotropy in its electronic properties and the presence of strong electron correlations.

DOI: 10.1103/PhysRevLett.89.086601

PACS numbers: 72.15.Gd, 74.72.Bk

The evolution of the electronic ground state with doping in a one-dimensional (1D) or two-dimensional (2D) Mott insulator is one of the most fundamental unresolved problems in solid state physics. Over the past decade or so, much work has focused understandably on the high- T_c superconductivity and the anomalous 2D metallic state that develops out of the Mott insulating phase of the undoped CuO_2 planes in high- T_c cuprates. However, in recent years, quasi-1D (Q1D) cuprates have also come to the fore.

Angle-resolved photoemission spectroscopy (ARPES) on the Q1D half-filled Mott insulators SrCuO_2 [1] and Sr_2CuO_3 [2] have provided arguably the clearest evidence to date of spin-charge separation, the hallmark of a 1D Luttinger liquid (LL). The CuO chains in Sr_2CuO_3 and SrCuO_2 are isostructural with the single- and double-chain networks found in $\text{YBa}_2\text{Cu}_3\text{O}_{7-\delta}$ (Y123) and $\text{YBa}_2\text{Cu}_3\text{O}_8$ (Y124), respectively. The intrinsic physics of the hole-doped chains, however, is obscured by the (super)conductivity in the CuO_2 planes. Only Pr substitution for Y suppresses in-plane conductivity without affecting the chains [3] and allows the low-energy excitations of the doped CuO chains to be studied in isolation.

Pr123, the quarter-filled analog of Sr_2CuO_3 , undergoes a CDW transition at 120 K [4], presumably driven by the strong electron correlations. In Pr124, the hole-doped analog of SrCuO_2 at 1/4 filling, several features of the optical spectra at 300 K [5] are compatible with LL behavior with an anomalous exponent $K_\rho \approx 0.24$ indicative of strong correlation effects comparable to those found in the Bechgaard salts $(\text{TMTSF})_2X$ ($X = \text{PF}_6, \text{ClO}_4$). ARPES [6], on the other hand, has revealed a large spectral weight near the Fermi level ε_F , consistent with reports of metallic resistivity down to low T [7,8], but could not show conclusive evidence for Fermi crossing. Indeed, other spectral features [6] were incompatible with a Fermi-liquid (FL) description and more reminiscent of the Q1D charged stripes seen in underdoped cuprates.

In this Letter, we report a detailed study of the interchain resistivity of Pr124 in high magnetic fields up to 30 T.

The agreement found between the magnetoresistance (MR), zero-field resistivity, and predictions of Boltzmann transport theory provides strong evidence that Pr124 is indeed a 3D FL at low T , albeit an extremely anisotropic one. Moreover, the temperature scale that defines the onset of coherent interchain hopping in Pr124 is shown to be comparable with the warping of the Q1D sheets, determined from the field-induced dimensional crossovers observed in both transverse directions. These two observations may be key to the development of a consistent theoretical model to describe the crossover from FL to LL in Q1D metals as temperature and/or interchain hopping t_\perp are varied.

Single crystals were flux-grown in high pressure oxygen [8]. Typical abc dimensions of crystals studied here were $0.2 \times 0.3 \times 0.05 \text{ mm}^3$. To measure the intrinsic interchain resistivity, 25 μm gold wires were painted onto the crystals in a quasi-Montgomery configuration appropriate for anisotropic samples. The MR measurements were carried out on one a -axis and two c -axis ($c\#1$ and $c\#2$) mounted crystals using a single-axis rotation stage, angular resolution 0.25° , placed inside a 32 T ^3He system.

The zero-field resistivity of Pr124 is shown in Fig. 1. The most striking feature of the data is the magnitude of ρ_a and the correspondingly large anisotropy for in-plane transport $\rho_a/\rho_b \sim 1000$ at 4.2 K, seemingly confirming the insulating character of the CuO_2 planes in Pr124 [3]. The chain resistivity $\rho_b(T)$ is metallic for all $T \leq 300$ K, while $\rho_a(T)$ and $\rho_c(T)$ show crossovers from metallic to semiconducting behavior with increasing T . $\rho(T)$ varies as T^2 along all three current directions below $T = 50$ K [9]. Significantly, with reference to elongated Pr123 [10], no superconductivity is observed down to 0.5 K. The residual b -axis resistivity ρ_{b0} is only 4 $\mu\Omega \text{ cm}$, giving a surprisingly long mean free path along the chains $\ell_b \sim 800 \text{ \AA}$. The ordering of the Pr ions at $T_N(\text{Pr}) = 17$ K is manifest as a kink in $\rho_c(T)$ but has a negligible effect on $\rho_b(T)$ and $\rho_a(T)$. $c\#1$ and $c\#2$ show similar $\rho_c(T)$ behavior but have different residual resistivities, $\rho_{c0} = 8.0$ and 11.5 $\text{m}\Omega \text{ cm}$,

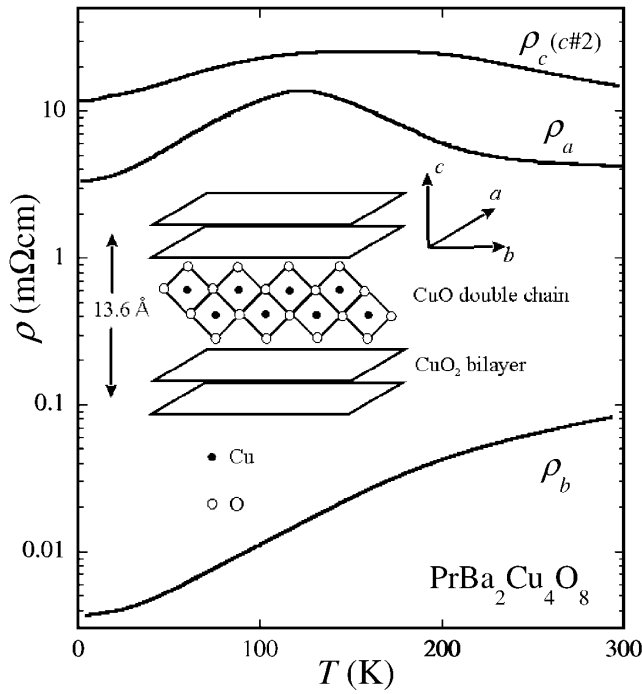


FIG. 1. Anisotropic zero-field resistivity of Pr124. Inset: Schematic of the crystal structure of Pr124.

respectively, indicating their different impurity concentrations, n_{imp} . Only $c\#2$ is shown in Fig. 1.

Figure 2 shows MR field sweeps up to 30 T for $I \parallel c$ ($c\#2$, top panel) and $I \parallel a$ (bottom panel) taken at $T = 0.5$ K. Note the striking anisotropy between the different field orientations. In particular, for $B \parallel a$, $\Delta\rho_c/\rho_c$ is extremely large, while $\Delta\rho_a/\rho_a$ is practically zero. Many features of the data are consistent, both qualitatively and quantitatively, with quasiclassical transport theory for a Q1D metal with open, slightly warped Fermi sheets. First, all transverse MR sweeps vary as B^2 in the weak-field limit ($B < 5$ T). Second, MR is largest for $B \perp I \perp b$ (i.e., when the Lorentz force is largest) and smallest (even negative) for $B \parallel b$ (i.e., when the field is parallel to the main velocity component v_b). With $B \parallel a$, $\Delta\rho_c/\rho_c$ ($c\#2$) $\sim 80\%$ at $B = 10$ T and $\sim 700\%$ at $B = 30$ T. (For $c\#1$, which has the lower ρ_{c0} and hence longer ℓ_b , $\Delta\rho_c/\rho_c \sim 1500\%$ at $B = 30$ T.) This is by far the largest MR ever observed in a cuprate. For a Q1D Fermi surface in the weak-field limit, Boltzmann transport theory gives $\Delta\rho_c/\rho_c$ ($B \parallel a$) = $(eBc/\hbar)^2 \ell_b^2$, where $c = 13.6$ Å is the c -axis lattice parameter. From the initial slope of the MR sweep, we obtain $\ell_b \sim 600$ and 400 Å for $c\#1$ and $c\#2$, respectively, in good agreement with the estimate obtained from ρ_{b0} . Similarly, for $I \parallel a$ ($B \parallel c$), $\Delta\rho_a/\rho_a = (eBa/\hbar)^2 \ell_b^2$, with $a = 3.8$ Å, and at $T = 0.5$ K we again find $\ell_b \sim 600$ Å.

The top panel of Fig. 3 shows the evolution of the transverse c -axis MR for both $c\#1$ (main figure) and $c\#2$ (inset) up to $T = 120$ K. The qualitative features of the data are identical for the two samples: $\Delta\rho_c(B)$ drops dramatically with increasing T , i.e., as ℓ_b decreases; $d\rho_c/dT$ is positive at low B and negative at high B , and

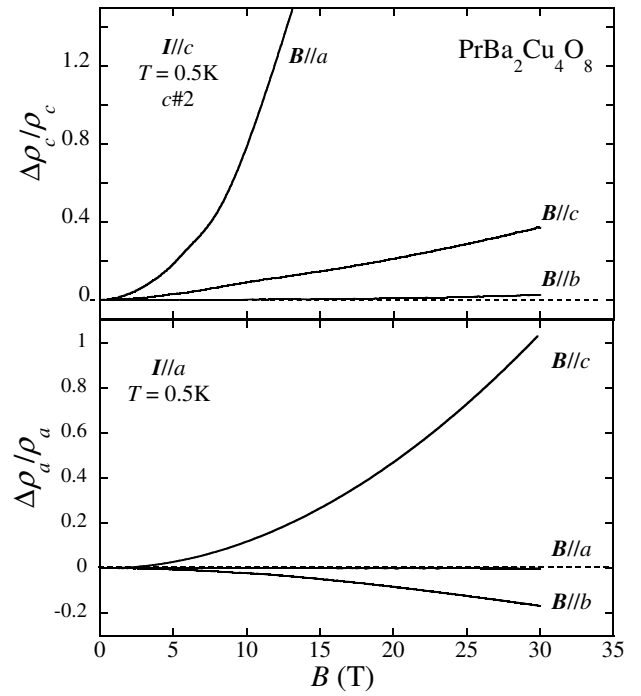


FIG. 2. MR field sweeps for $I \parallel c$ ($c\#2$, top panel) and $I \parallel a$ (bottom panel) in different field orientations.

the B dependence becomes weaker at higher fields. The bottom panel of Fig. 3 shows the resultant $\rho_c(T, B)$, obtained by plotting the value of ρ_c at fixed B and different T . Note that the minimum in $\rho_c(T)$ shifts to higher T with increasing field.

Similar behavior has also been observed in Y124 [11] ($T > T_c$) and in $(\text{TMTSF})_2\text{X}$ [12,13] and attributed to a field-induced dimensional crossover arising from the slightly warped nature of the Q1D Fermi sheets. In Pr124, for $B \parallel a$, the dominant Lorentz force is directed along the c axis. This gives rise to an oscillatory c -axis component to the real-space quasiparticle trajectory with an amplitude $A_c = 4t_c/e v_b B$. As B increases, A_c shrinks until eventually the carriers become confined to a single plane of coupled chains once $A_c \sim c$ [14]. In other words, t_c is renormalized in the presence of a perpendicular field. Note that this expression is independent of the intrachain scattering rate, implying that the decoupling field should be independent of T and n_{imp} .

More insight into the nature of the field-induced dimensional crossover can be learned from the derivatives $d\rho_c/dB$, as shown in Fig. 4. At the lowest T , two distinct features emerge; a peak at $B = 5.5$ T (marked by a dotted line) and a more gradual though still distinct crossover to a weaker field dependence centered around $B = 11$ T (also marked by a dotted line and located by the intersection of the slopes of $d\rho_c/dB$ above and below 11 T). The first peak gradually becomes smeared out and disappears above $T = 40$ K, while the latter feature persists up to 90 K. Above 90 K, $\rho_c(B) \sim B^2$ up to 30 T. Also shown in Fig. 4 for comparison is $d\rho_c/dB$ for $c\#1$ at $T = 0.5$ K. Apart from

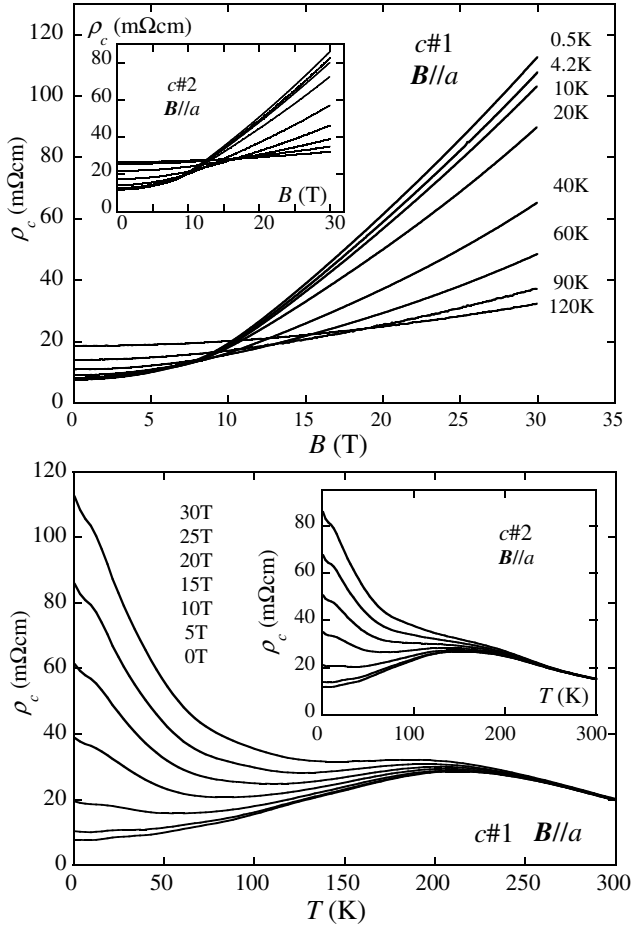


FIG. 3. Top panel: c -axis MR field sweeps for $c1$ up to 30 T with $\mathbf{B} \parallel a$. Inset: Corresponding sweeps for $c2$. Bottom panel: $\rho_c(T, B)$ curves for $c1$ at different fields ($\mathbf{B} \parallel a$) obtained directly from the MR field sweeps. Inset: Corresponding $\rho_c(T, B)$ curves for $c2$.

their magnitudes, the features observed in the two crystals are identical in every respect.

The two features observed in $d\rho_c/dB$ are independent of both temperature and disorder (recall that $c\#1$ and $c\#2$ have significantly different ℓ_b), consistent with the dimensional-crossover scenario described above. Because of hybridization effects, the separate sheets of the double CuO chain unit in Pr124 will have slightly different k_F values and likewise different warpings in the two transverse directions, as calculated for Y124 [15]. We therefore attribute these two features to the individual crossover fields B_{cr}^c for the two separate pairs of chain sheets in Pr124. A change in $d\rho_c/dB$ at B_{cr}^c was also observed in Y124 [11], though in that case, only one crossover field was visible, presumably due to the elevated temperatures ($T > T_c \sim 80$ K). Given $v_b \sim 2.5 \times 10^5$ ms $^{-1}$ [6], we obtain an estimate for the c -axis warping $4t_c$ on the two sheets in Pr124 of 2 meV (~ 23 K) and 4 meV (~ 45 K). These estimates are consistent with the smearing of the features seen in $d\rho_c/dB$ beyond $k_B T = 4t_c$ and also with the deviation from $\rho_c(T) \sim T^2$ above $T = 50$ K that signals the crossover from coherent to incoherent c -axis transport [9].

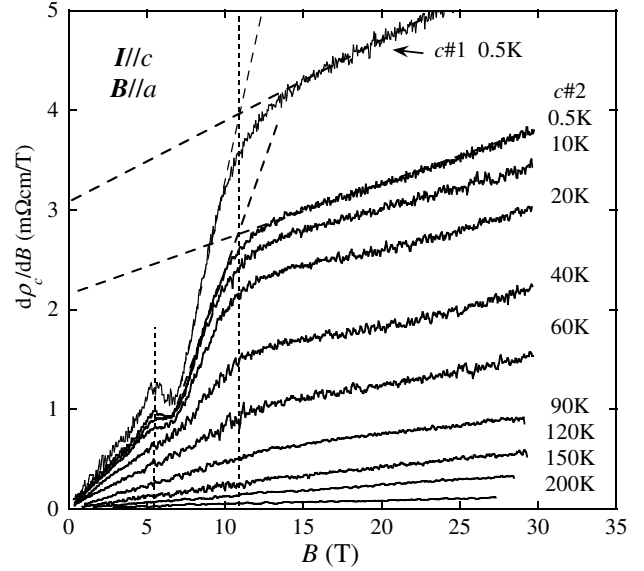


FIG. 4. $d\rho_c/dB$ for $c2$ for $0.5 \text{ K} \leq T \leq 200 \text{ K}$. $d\rho_c/dB$ for $c1$ at $T = 0.5 \text{ K}$ (top curve) is also shown for comparison. The dashed and dotted lines are explained in the text.

A similar coherent/incoherent crossover is also expected to occur in the reciprocal configuration $\mathbf{I} \parallel a$ and $\mathbf{B} \parallel c$ once the amplitude of oscillation of the real-space trajectory along the a -axis $A_a = 4t_a/e v_b B \leq a$. Figure 5 shows the transverse a -axis MR sweeps up to 30 T ($\mathbf{B} \parallel c$) for $1.5 \text{ K} \leq T \leq 85 \text{ K}$ (shown as solid lines). No crossover is observed up to 30 T, and no features are observed in $\rho_a(B)$. Indeed, $\rho_a(B) \sim B^2$ for the entire experimental field range. However, by extrapolating this B^2 dependence to higher fields (dashed lines in Fig. 5), we find that all field sweeps eventually converge to a single point at $B \sim 60$ T. $d\rho_a/dT$ is negative (positive) above (below) 60 T, respectively, indicating a second dimensional crossover. We ascribe this convergence to the crossover field for a -axis hopping B_{cr}^a and obtain an estimate for $4t_a = e v_b B_{cr}^a a = 6$ meV (70 K). Again this is consistent with the onset temperature ($T_a^{\text{coh}} = 75$ K) for incoherent transport along the a axis (inferred from the deviation from T^2 resistivity) shown in the inset of Fig. 5. Note that since $a \sim c/4$, a much higher field is required to decouple the chains in the a direction.

This ubiquitous agreement between the interchain (magneto)transport behavior in Pr124 and quasiclassical transport theory is the central result of this Letter. While the transport properties of a LL are not well defined at present, thus making it difficult to rule out a LL ground state on quantitative grounds, it should be borne in mind that a key component of Boltzmann transport theory is the delta function in the momentum distribution function at ε_F which is absent in the LL. The internal consistency with Boltzmann transport analysis, coupled with the observation of a T^2 resistivity along all three axes, should therefore be viewed as collective evidence for the development of a FL ground state in this strongly correlated Q1D cuprate at low T . The ratio of the hopping parameters ($t_b^2 : t_a^2 : t_c^2 \sim 2500 : 2 : 1$) makes Pr124 one of the most 1D metals ever to

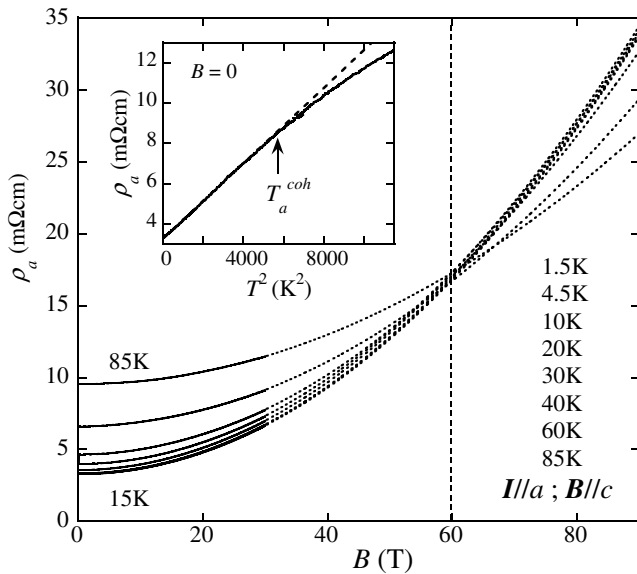


FIG. 5. a -axis transverse MR up to 30 T with $\mathbf{B} \parallel c$ (solid lines). The dashed lines are extrapolations of the B^2 dependence up to 90 T. The dotted line represents the predicted B_{cr} for $\mathbf{I} \parallel a$. Inset: Low T zero-field $\rho_a(T)$ data plotted versus T^2 . The arrow indicates the deviation from T^2 at $T \sim 75$ K.

have been characterized [16]. In this sense, our observations confirm predictions from renormalization group theory that any finite t_{\perp} will stabilize a 3D FL ground state in a Q1D conductor [17]. This contrasts with the bosonization approach [18], for example, which argues that for sufficiently small t_{\perp} , the system should exhibit LL behavior with anomalous scaling similar to that expected for $t_{\perp} = 0$. The low values of t_{\perp} in Pr124 appear to set an upper bound on the applicability of the bosonization model.

A deviation from $\rho_{\perp}(T) \propto T^2$ at $k_B T \sim 4t_{\perp}$ was also observed in the Q2D FL Sr_2RuO_4 (with $4t_{\perp}$ determined by quantum oscillations [19]). In Q1D conductors, however, this crossover is believed to be strongly renormalized through interactions [20]. The small values of t_a and t_c obtained here may suggest some renormalization of the interchain hopping in Pr124, but any quantitative analysis must await detailed band structure calculations.

Surprisingly, and despite the extreme anisotropy of Pr124, the field-induced one-dimensionalization does not lead to a charge/spin ordered state, as frequently observed in Q1D metals. Various possible explanations for the lack of an ordering transition in Pr124 have been proposed, including the effect of weak hopping *between* the individual CuO chains (that removes the tendency towards nesting), deviations from commensurate $1/4$ filling [6], and geometric frustration in the CuO double chain [21]. Whatever the reason, this lack of ordering makes Pr124 an ideal laboratory for testing theoretical predictions of electronic ground states in low-dimensional conductors, since 1D, 2D, and 3D transport can all be observed in Pr124 at ambient pressures through varying T , B , and n_{imp} [9,22]. More-

over, for appropriately tilted fields above both B_{cr}^a and B_{cr}^c , all mobile carriers in Pr124 should become confined to an individual double-chain unit, thus opening up a possible avenue to purely 1D metallic transport in a 3D solid.

In conclusion, we have shown that the CuO double chains in Pr124 form an anisotropic 3D FL ground state at low T and have characterized the warping of the Q1D sheets through the observation of two magnetic-field-induced dimensional crossovers in orthogonal fields. Coupled with the recent observation of the Wiedemann-Franz law in overdoped $\text{Tl}_2\text{Ba}_2\text{CuO}_{6+\delta}$ [23], we now have strong experimental support for a stable FL fixed point in both the hole-doped 1D and 2D cuprates. Given that spin-charge separation has already been established for the half-filled Mott insulating phase in 1D cuprates (but intriguingly *not* in 2D cuprates), experiments that probe the crossover between these two fundamentally extreme ground states should prove highly revealing.

We acknowledge helpful discussions with K. Behnia, S. J. Blundell, and A. T. Boothroyd. This work was partially supported by EPSRC, Grant No. GR/R35995/01. S. H. was financially supported by the Japan Society for the Promotion of Science (JSPS).

- [1] C. Kim *et al.*, Phys. Rev. Lett. **77**, 4054 (1996).
- [2] H. Fujisawa *et al.*, Phys. Rev. B **59**, 7358 (1999).
- [3] R. Fehrenbacher and T. M. Rice, Phys. Rev. Lett. **70**, 3471 (1993).
- [4] B. Grevin *et al.*, Phys. Rev. Lett. **80**, 2405 (1998).
- [5] K. Takenaka *et al.*, Phys. Rev. Lett. **85**, 5428 (2000).
- [6] T. Mizokawa *et al.*, Phys. Rev. Lett. **85**, 4779 (2000).
- [7] I. Terasaki *et al.*, Phys. Rev. B **54**, 11 993 (1996).
- [8] S. Horii *et al.*, Phys. Rev. B **61**, 6327 (2000).
- [9] M. N. McBrien *et al.*, J. Phys. Soc. Jpn. **71**, 701 (2002).
- [10] Z. Zou, J. Ye, K. Oka, and H. Nishihara, Phys. Rev. Lett. **80**, 1074 (1998).
- [11] N. E. Hussey *et al.*, Phys. Rev. Lett. **80**, 2909 (1998).
- [12] K. Behnia *et al.*, Phys. Rev. Lett. **74**, 5272 (1995).
- [13] E. I. Chashechkina and P. M. Chaikin, Phys. Rev. Lett. **80**, 2181 (1998).
- [14] L. P. Gorkov and A. G. Lebed, J. Phys. (Paris), Lett. **45**, L433 (1984).
- [15] J. Yu, K. T. Park, and A. J. Freeman, Physica (Amsterdam) **172C**, 467 (1991).
- [16] The interchain bandwidth $t_b \sim 100$ meV in $(\text{TMTSF})_2\text{X}$.
- [17] C. Castellani, C. Di Castro, and W. Metzner, Phys. Rev. Lett. **69**, 1703 (1992).
- [18] P. Kopietz, V. Meden, and K. Schonhammer, Phys. Rev. Lett. **74**, 2997 (1995).
- [19] A. P. Mackenzie *et al.*, Phys. Rev. Lett. **76**, 3786 (1996).
- [20] A. Georges, T. Giamarchi, and N. Sandler, Phys. Rev. B **61**, 16 393 (2000).
- [21] H. Seo and M. Ogata, Phys. Rev. B **64**, 113103 (2001).
- [22] K. Nakada *et al.*, Physica (Amsterdam) **357C**, 186 (2001).
- [23] C. Proust *et al.*, cond-mat/0202101.